Gene 592 (2016) 86–98

Contents lists available at ScienceDirect

Gene

journal homepage: www.elsevier.com/locate/gene

Research paper

Differentiation-inducing and anti-proliferative activities of isoliquiritigenin and all-trans-retinoic acid on B16F0 melanoma cells: Mechanisms profiling by RNA-seq

Xiaoyu Chen [a,1], Ming Yang [b,1], Wenjin Hao [c], Jichun Han [c], Jun Ma [c], Caixia Wang [d], Shiguo Sun [a,*], Qiusheng Zheng [c,**]

[a] College of Science, Northwest A&F University, Yangling, Shaanxi 712100, China
[b] BGI-Tech, BGI-Shenzhen, Shenzhen, Guangdong 518083, China
[c] Binzhou Medical University, Yantai, Shandong 264003, China
[d] Key Laboratory of Coastal Biology and Bioresource Utilization, Yantai Institute of Coastal Zone Research, Chinese Academy of Sciences, Yantai 264003, China

ARTICLE INFO

Article history:
Received 17 February 2016
Received in revised form 14 July 2016
Accepted 22 July 2016
Available online 25 July 2016

Keywords:
Isoliquiritigenin
All-trans-retinoic acid
Melanoma
Differentiation
RNA-seq
ROS

ABSTRACT

Melanoma is a cancer that arises from melanocytes, specialized pigmented cells that are found predominantly in the skin. The incidence of malignant melanoma has significantly increased over the last decade. With the development of therapy, the survival rate of some kind of cancer has been improved greatly. But the treatment of melanoma remains unsatisfactory. Much of melanoma's resistance to traditional chemotherapy is believed to arise intrinsically, by virtue of potent growth and cell survival-promoting genetic alteration. Therefore, significant attention has recently been focused on differentiation therapy, as well as differentiation inducer compounds. In previous study, we found isoliquiritigenin (ISL), a natural product extracted from licorice, could induce B16F0 melanoma cell differentiation. Here we investigated the transcriptional response of melanoma differentiation process induced by ISL and all-trans-retinoic acid (RA). Results showed that 390 genes involves in 201 biochemical pathways were differentially expressed in ISL treatment and 304 genes in 193 pathways in RA treatment. Differential expressed genes (DGEs, fold-change (FC) ≥ 10) with the function of anti-proliferative and differentiation inducing indicated a loss of grade malignancy characteristic. Kyoto Encyclopedia of Genes and Genomes (KEGG) pathway analysis indicated glutathione metabolism, glycolysis/gluconeogenesis and pentose phosphate pathway were the top three relative pathway perturbed by ISL, and mitogen-activated protein kinase (MAPK) signaling pathway was the most important pathway in RA treatment. In the analysis of hierarchical clustering of DEGs, we discovered 72 DEGs involved in the process of drug action. We thought Cited1, Tgm2, Xaf1, Cd59a, Fbxo2, Adh7 may have critical role in the differentiation of melanoma. The evidence displayed herein confirms the critical role of reactive oxygen species (ROS) in melanoma pathobiology and provides evidence for future targets in the development of next-generation biomarkers and therapeutics.

1. Introduction

Melanoma represents a largely unsolved challenge for radio/chemotherapy of malignant disease because of the intrinsic/extrinsic resistance of melanoma cells. Nevertheless, the mechanisms underlying such a radio/chemo-resistant cell phenotype remain mostly unknown (Bajetta et al., 2002). Thus, looking for effective ways to control the occurrence, development of melanoma is pressing (Facchetti et al., 2007). Tumor differentiation is a modality aimed at re-activating endogenous differentiation programs in cancer cells and induces cancer cells to stop proliferating and to express characteristics of normal cells. Differentiation therapy is different from radio/chemotherapy by its less toxic and drug resistance. Early successes in "differentiation therapy" were achieved in the treatment of promyelocytic leukemia with retinoic acid (Sell, 2005). But less development of differentiation-based therapy are found in solid tumours. In the case of melanoma, a number of cell lines thought to represent 'blocked' stages of melanoma differentiation have been isolated and studied (Herlyn et al., 1985; Herlyn et al., 1980;

Abbreviations: ROS, reactive oxygen species; RA, all-trans-retinoic acid; ISL, isoliquiritigenin; DGEs, differential expressed genes; DMSO, dimethyl sulfoxide; a-MSH, cAMP-elevating agents such as a melanocyte-stimulating hormone; MITF, microphthalmia-associated transcription factor; GO, Gene Ontology; KEGG, Kyoto Encyclopedia of Genes and Genomes.

* Correspondence to: S. Sun, The Northwest A&F University, Yangling 712100, China.
** Correspondence to: Q. Zheng, The Binzhou Medical University, Yantai 264003, China.
E-mail addresses: sunsg@nwsuaf.edu.cn (S. Sun), zqsyt@sohu.com, johnsonjem@hotmail.com (Q. Zheng).

[1] These authors contributed equally to this work.

http://dx.doi.org/10.1016/j.gene.2016.07.052
0378-1119/

Watkins et al., 1982). Discovery of new cancer-specific differentiation inducers and elucidation of the mechanism underlying cancer cell differentiation holds promise for developing improved therapies for melanoma (Barres & Dugas, 2008; Krissansen et al., 2003).

The mouse melanoma cell line B16 was isolated from C57 BL/6 mice (Potop et al., 1984). Some studies demonstrated that B16 cells can be induced to differentiate into mature melanocyte-like cells by treatment with dimethyl sulfoxide(DMSO), dimethyl thiourea, sodium butyrate, histidinol (Nordenberg et al., 1985; Nordenberg et al., 1986; Nordenberg et al., 1987; Nordenberg et al., 1989; Nordenberg et al., 1990), cAMP-elevating agents such as a melanocyte-stimulating hormone (a-MSH) (Engan et al., 1995), signal transduction pathway inhibitors (Buscà et al., 1996), mannosylerythritol lipid (Zhao et al., 2001), Alteronol (Wang et al., 2015) and all-trans-retinoic acid (RA) which is widely used as a differentiation inducer (Estler et al., 2008). However, compounds tested so far did not seem to be suitable for immediate clinical evaluation except RA. Natural products and their derivatives which possess the advantages of hypotoxicity and extensive material have historically been invaluable as a source of therapeutic agents (Liu, 2004; Walle & Halushka, 2001; Park et al., 2008). The past few years, however, have seen a renewed interest in the use of natural compounds and, more importantly, their role as a differentiation inducer (Amin & Buratovich, 2007; Liu et al., 2010a; Robles-Fernández et al., 2013). Some natural products like Theophylline (Kreider et al., 1975a), lupane triterpenes (Hata et al., 2006), 5,7-dimethoxycoumarin (Alesiani et al., 2008) have showed the activity of inducing tumor differentiation. The modern tools of chemistry and biology-in particular, the various '-omics' technologies, now allow scientists to detail the exact nature of the biological effects of natural compounds on the human body, as well as to uncover possible synergies, which holds much promise for the development of differentiation therapy against many devastating diseases, including melanoma.

The resistance of melanoma to existing treatment modalities and the rapid rise in its incidence (Lens & Dawes, 2004; Beddingfield, 2003) underscore the importance of acquiring a better understanding of the pathogenesis of this disease. Melanoma progression and metastasis is traditionally modeled as a stepwise process with the initial mutagenic event occurring in a melanocyte in the epidermis, with further mutation resulting in the proliferation passing through nevus and dysplastic nevus phases. It is reported by research that reveals melanocytes can be transformed with oncogenes and acquire malignant/invasive characteristics (Chudnovsky et al., 2005). Furthermore, the tyrosinase promoter, expressed in melanocytes, has been shown to induce melanoma when driving oncogenic proteins SV40E (Kelsall & Mintz, 1998) and N-Ras (Atkinson et al., 2015). Evidence supports the presence of melanoma stem-like cells (Fang et al., 2005; Roesch, 2015). First, melanomas show phenotypic heterogeneity both in vivo and in vitro, suggesting an origin from a cell with multilineage differentiation abilities (Grichnik et al., 2006). Second, melanoma cells often express developmental genes (Liu et al., 2014). Third, melanoma cells can differentiate into a wide range of cell lineages, including neural, mesenchymal, and endothelial cells (Reed et al., 1999; Fang et al., 2001). Studies on metastatic melanoma lines have revealed that melanomas are believed to arise from a mature, differentiated melanocyte. Evidence also indicated an existence of re-differentiation for melanoma self-renewal that drives tumorigenesis. An early study revealed that theophylline involved in the regulation of B16 melanoma cells proliferation and differentiation, the theophylline-treated cells contained ten times the melanin and an elevated cAMP content compared to the controls (Kreider et al., 1975b); subsequent studies showed that DMSO also showed antiproliferative and differentiating effects; vitamin A (retinoids) regulated mouse melanoma growth and differentiation, induces a six-fold to eight-fold increase in protein kinase C (PKC) α RNA and protein, which is not a direct target of retinoic acid (RA). It has been proposed that melanoma cells intrinsically possess a genetic programme predisposing them to exacerbated metastatic features (Gupta et al., 2005). The most remarkable gene is the microphthalmia-associated transcription factor (MITF), which is the key molecular switch between mouse or human melanoma initiating cells and their differentiated progeny. Indeed, MITF was identified as the master gene in melanocyte differentiation, which it does by controlling the expression of melanogenic enzymes (TYR, TYRP1, DCT). Later, MITF was shown to regulate the expression of genes involved in all steps of melanocyte differentiation, including dendricity (DIA), melanosome biogenesis (SILVER, OA1) and melanosome transport (RAB27a) (Cheli et al., 2011). Concomitantly, King et al. (2001) reported that MITF expression was maintained in >85% of melanoma, and a MITF gene amplification has been found in >20% of metastatic melanomas. As is the case for many other neoplasms, physiological differentiation of melanocytes and metastatic melanoma development share common signaling pathways, such as ERK and PI3 kinase pathways (King et al., 2001). Many of these changes, originally discovered through examination of tumor biopsies, have been functionally validated using experimental models. But in this way researchers may cost too much but gain little. Estler et al. (2008) invited microarray to determine gene expression changes during retinoic acid-induced growth arrest and differentiation of melanoma to gain a globe knowledge of RA "normalized" the expression of genes involved in energy metabolism, DNA replication, DNA repair and differentiation. With the help of microarray, researchers may get an easier process to study the mechanism of pharmacological effects of drugs. Over the past 10 years, introduction of high-throughput next-generation sequencing (NGS) technologies have revolutionized transcriptomics by providing opportunities for multidimensional studies of cellular transcriptomes. Thus, it becomes possible because large-scale expression data are acquired at a single-base resolution. As a main quantitative transcriptome profiling platform, RNA-seq has been considered a new experimental method to replace microarray.

In our previous study, we have found isoliquiritigenin (ISL) derived from traditional Chinese medicine licorice could induce the differentiation in mouse melanoma B16F0 cells (Liu et al., 2010b; Wang et al., 2010a; Wang et al., 2010b). But we only profiled the role of reactive oxygen species (ROS) during ISL induced B16F0 cell differentiation. To gain additional insight into the molecular alterations and cellular events of melanoma differentiation, we performed the transcriptome profiling analysis of ISL/RA induced B16F0 cell differentiation using RNA-Seq.

2. Materials and methods

2.1. Cell line and cell culture

B16F0 cells were purchased from China Center for Type Culture Collection (CCTCC, Wuhan, China). The cells were maintained in RPMI 1640 medium supplemented with 10% fetal bovine serum, and 100 U/mL penicillin, 100 μ g/mL streptomycin at 37 °C with 5% CO_2. The cells were split every 2 day and were diluted 1 day before each experiment.

2.2. Preparation of a cDNA library for RNA-Seq

Total RNA was extracted from untreated (C) or isoliquiritigenin/all-trans-retinoic acid (ISL/RA) treated B16F0 cells using TRIzol® reagent (Invitrogen, Burlington, ON, Canada) and then treated with DNase to remove potential genomic DNA contamination according to the manufacturer's protocol. The yield and purity of RNA were assessed by determination of the absorbance (Abs) at 260 and 280 nm. RNA was only used when the Abs260 nm/Abs280 nm ratio was >1.8. RNA integrity was checked using a 1% agarose gel with the RNA 6000 Nano Assay Kit and Agilent 2100 Bioanalyzer. The extracted total RNA was stored at −70 °C for later use.

The total RNA was extracted and mRNA of B16F0 cells was enriched by using the oligo(dT) magnetic beads. Adding the fragmentation buffer, the mRNA was interrupted to short fragments (about 200 bp), then the first strand cDNA was synthesized by random hexamer-primer

using the mRNA fragments as templates, then added dNTPs, RNase H and DNA polymerase I to synthesize the second strand. The double-stranded cDNA was purified with QiaQuick PCR extraction kit and washed with EB buffer for end repair and single nucleotide A (adenine) addition. Finally, sequencing adaptors were ligated to the fragments. The required fragments was purified by agrose gel electrophoresis and enriched by PCR amplification. The library products was sequenced and 50 bp sequences were generated via the Illumina sequencing platform (HiSeqTM 2000).

2.3. Mapping reads to the reference genome and differential expression (DE) detection, differential gene expression analysis and clustering

Prior to mapping reads to the reference database (NCBI37/mm9), we filtered all reads to remove adaptor reads and low-quality reads (the percentage of quality value ≤5 bases was >50% in a read) before data analysis. The remaining reads were mapped to the reference gene set using SOAPaligner/soap2 (Li et al., 2009), allowing up to two base mismatches.

To obtain normalized gene expression levels, we calculated reads by the reads per kb per million reads (RPKM) method (Mortazavi et al., 2008). The cutoff value for determining gene transcriptional activity was determined based on a 95% confidence interval for all RPKM values for each gene. A previous described rigorous significance test (Audic & Claverie, 1997), with some modifications by BGI-Shenzhen company was utilized to identify significant differentially expressed genes between two samples. Also, the false discovery rate was calculated based on the methods published by Benjamini Y and Yekutieli D (Benjamini & Yekutieli, 2001). We used false discovery rate (FDR) ≤ 0.001 and the absolute value of $\log_2$Ratio ≥ 1 as the threshold to judge the significance of gene expression difference (Storey and Tibshirani, 2003).

For an optimal comparison of the results, hierarchical clustering was performed to identify candidate genes involved in specific gene expression patterns using with cluster 3.0 software (de Hoon et al., 2004) and Java Treeview (Saldanha, 2004). The parameter of cluster 3,0 used in this research are "-g 7 -e 7 –m a". The similarities between gene expression data was measured by Euclidean distance. 2D clustering diagram was used to compare gene expression levels for C-vs-ISL and C-vs-RA.

2.4. Quantitative PCR (qPCR) analysis

In order to verify the DGE results, we used qPCR analysis. The RNA samples used for the qPCR assays were both the same as for the DGE experiments and independent RNA extractions from biological replicates. qPCRs were done on the Lightcycler480 (Roche), with SYBR-Green detection (SYBR PrimeScript RT-PCR Kit, TaKaRa Biotechnology Co., Ltd.), according to the manufacture's instruction. Each cDNA was analyzed in triplicate, after which the average threshold cycle (Ct) was calculated per sample. The relative expression levels were calculated with the $2^{-\Delta\Delta Ct}$ method. The results were normalized to the expression level of Glyceraldehyde-3-phosphate dehydrogenase (GAPDH) and relative to the C sample (control group: B16F0 cells treated without drugs).

2.5. Gene Ontology (GO) analysis

Gene Ontology (GO) is an international standardized gene functional classification system which offers a dynamic-updated controlled vocabulary and a strictly defined concept to comprehensively describe properties of genes and their products in any organism. GO has three ontologies: molecular function, cellular component and biological process. The basic unit of GO is GO-term. Every GO-term belongs to a type of ontology.

GO enrichment analysis provides all GO terms that significantly enriched in DEGs comparing to the genome background, and filter the DEGs that correspond to biological functions. The DAVID web tool (http://david.abcc.ncifcrf.gov/) was used to identify significantly enriched GO terms among the given list of genes that are differentially expressed (Huang da et al., 2009). The *p*-value analyzed by DAVID goes through Bonferroni Correction, taking corrected *p*-value ≤0.05 as a threshold. GO terms fulfilling this condition are defined as significantly enriched GO terms in DEGs. This analysis is able to recognize the main biological functions that DEGs exercise. GO categories with *p*-value <0.01 were considered significant.

2.6. Pathway analysis of differential expression genes(DEGs)

Pathway analysis is mainly based on the Kyoto Encyclopedia of Genes and Genomes (KEGG) database. Two-side Fisher's exact test with a multiple testing was used to analysis pathway enrichment, which identified significantly enriched metabolic pathways or signal transduction pathways in DEGs comparing with the whole genome background. The calculating formula is the same as that in GO analysis. Here N is the number of all genes that with KEGG annotation, n is the number of DEGs in N, M is the number of all genes annotated to specific pathways, and m is number of DEGs in M. We chose only pathway categories that had a Q-value ≤ 0.05.

3. Results

3.1. Illumina sequencing and aligning to the reference genome

An immediate application of our RNA sequence data included gene expression profiling at cells treated with or without drug. RNA-seq was employed to analyze variations in gene expression of the B16F0 melanoma cell transcriptome. We sequenced three cDNA libraries (C, ISL and RA) using Illumina (single-end) sequencing technology, and obtained a total of 19.38 million raw reads with an average length of 50 bp, a total of approximately 968.98 million base pairs (Mbp). After removal of adaptor sequences, ambiguous reads and low-quality reads in which the percentage of unknown bases (N) is >10% and the percentage of the low-quality base (base with quality value ≤5) is >50%, a total of 5,925,877 (C) and 6,136,095 (ISL) and 5,896,974 (RA) high-quality clean reads comprised of 290,367,973 nucleotides (290 M) and 300,668,655 nucleotides (300 M) and 288,951,726 nucleotides (288 M) were generated from the C, ISL and RA libraries, respectively. These short reads were aligned to the mouse reference gene sequences and mouse reference genome sequences (mm9) using SOAPaligner/SOAP2 (Li et al., 2009). Of the total reads in 3 samples, 85.83% matched either to a unique (67.35%) or to multiple (18.48%) genomic locations; the remaining 14.17% were unmatched (Table 1), because only reads aligning entirely inside exonic regions will be matched (reads from exon-exon junction regions will not match).

3.2. Global analysis of gene expression

One of the primary goals of RNA-seq is to compare gene expression levels between samples. Based on the numbers of reads mapped to every gene in the reference database, we measured gene expression in reads per kilobase per million mapped sequence reads (RPKM), a normalized measure of read density described in RPKM method (Mortazavi et al., 2008).

A total of 12,877 (C), 13,121 (ISL) and 12,945 (RA) genes were detected in the samples. The removal of partial overlapping sequences yielded 12,031 genes, providing abundant data for the analysis of ISL or RA induced melanoma differentiation process. Their expression in the three cDNA libraries is summarized in Fig. 1 Venn diagram shows the distribution of expressed genes from C (control B16F0 melanoma cell), ISL (ISL treated B16F0 melanoma cell), and RA (RA treated B16F0 melanoma cell). Among these genes, 286 were co-expressed in C and ISL, 219 were co-expressed in C and RA, and 316 were co-expressed in ISL and RA. The number of specifically expressed genes was 488 (C), 379 (ISL), and 341 (RA), respectively.

Table 1
Summary of read numbers based on the RNA-Seq data from C, ISL and RA.

	Map to genome sequence		
	C	ISL	RA
Total reads	5,925,877	6,136,095	5,896,974
Mapped reads	5,075,613 (85.65%)	5,268,397 (85.86%)	5,070,171 (85.98%)
Unique match	3,978,578 (67.14%)	4,127,930 (67.27%)	3,989,517 (67.65%)
Multi-position match	1,097,035 (18.51%)	1,140,467 (18.59%)	1,080,654 (18.33%)
Unmapped reads	850,264 (14.35%)	867,698 (14.14%)	826,803 (14.02%)

3.3. Differential expression genes (DEGs) after ISL or RA treatment

To identify genes showing significant change in expression during different drug treatment, the differentially expressed genes after ISL or RA treatment were detected based on the criteria of significance (FDR ≤ 0.001 and $\log_2$ratio ≥ 1) (Marioni JC et al., 2008). As a result, a total of 487 significantly changed genes were detected between the C and ISL, of which 332 and 155 were found to be up-regulated and down-regulated, respectively (Fig. 2 and Table S1). Meanwhile, between the C and RA, there were 368 DEGs that were significantly differentially expressed, with 234 up-regulated and 134 down-regulated (Fig. 2 and Table S2). This suggests that the number of differently expressed genes between C and ISL is larger than that between C and RA. Between the R and ISL libraries, a total of 579 DEGs were detected, with 321 up-regulated genes and 258 down-regulated genes (Fig. 2 and Table S3). And the 10 most up- and down-regulated genes treated after ISL or RA are listed in Tables 2 and 3.

3.4. Validation of DGEs data by qPCR

To validate DE genes identified by Solexa sequencing, we randomly selected 6 genes for qPCR confirmation. The set included two down-regulated genes(Creb5, Cd74)and four up-regulated genes (Gsta3, Fcna, Efhd1, Spint1). Data were presented as fold changes in gene expression normalized to the GAPDH gene and relative to the C sample. Virtually all the genes show concordant direction of fold change between RNA-seq and qPCR. (Fig. 3). qPCR analysis (both pooling samples and independent RNA extractions from biological replicates) confirmed the direction of change detected by RNA-seq analysis. This correlation indicated the reliability of RNA-seq results. The primers used in qPCR analysis were showed in Table S4.

Fig. 1. Venn diagram showing the genes expressed in each of the three samples (ISL, RA and C). Among these genes, 12,031 are expressed at all three samples, 286 are co-expressed in ISL and C, 219 are co-expressed in RA and C, and 316 are co-expressed in ISL and RA. The number of sample-specifically expressed genes is 488 (ISL), 379 (RA), and 341(C), respectively.

3.5. Clustering of DEGs in different drug treatment

Genes with similar expression patterns usually have same functional correlation, so we went further cluster analysis based on the k-means method using Pearson's correlation distance, so that we could determine the similarity in relative change for each transcript across the set of different drug treatment, and how those changes were similar or differed between transcripts. These data were then subjected to hierarchical clustering using the Pearson correlation as the distance metric (Fig. 4 & Table S5).

Two-dimensional hierarchical clustering classified 72 differential expression (intersection between C-VS-ISL and C-VS-R) profiles into two expression cluster groups (Clusters 1 and Clusters 2) according to the similarity of their expression profiles, representing the number of profiles indicated using figure of merit analysis. Clusters 1 contained genes negatively modulated throughout the ISL or RA treatment, while genes expressed in Clusters 2 showed positively or negatively modulated in the ISL or RA treatment. Clusters 1, with 30 genes whose expression showed a similarity of their expression profiles, and among these 10 genes differently modulated during the treatment of ISL or RA. Cluster 2 was composed of 42 genes that positively modulated. The cluster analysis showed that ISL and RA has different regulatory pattern.

3.6. Functional analysis of DEGs during ISL or RA treatment based on RNA-seq data

To better characterize the effects of ISL and RA in biological processes we conducted GO enrichment analysis using DAVID (Bonferroni-corrected, FDR ≤ 0.05), with differentially expressed genes. Based on sequence homology, 434 and 340 DEGs could be categorized into 232 and 278 functional groups during ISL treatment and RA treatment (Fig. 5 and Table S6). In the three main categories (biological process, cellular component and molecular function) of the GO classification, there were 150, 29 and 53 functional groups with ISL treatment and 210, 34 and 34 functional groups with RA treatment, respectively (Fig. 5). Among these groups, the GO terms glucose metabolic process (GO: 0006006) in the biological process categories and response to stimulus in the biological process positive regulation of apoptosis (GO: 0043065) were both dominant in the treatment both of ISL and RA. We also noticed a high percentage of genes from oxidation reduction (GO: 0055114), cell death (GO: 0008219), death (GO: 0016265), apoptosis (GO: 0006915) and three glycometabolism process (glucose metabolic process, GO:0006006; hexose metabolic process, GO:0019318; monosaccharide metabolic process, GO:0005996) with the treatment of ISL. And a high percentage of genes from regulation of transcription from RNA polymerase II promoter (GO: 0006357), regulation of apoptosis (GO: 0042981), regulation of programmed cell death (GO: 0043067), regulation of cell death (GO: 0010941) and negative regulation of biosynthetic process (GO: 0009890) with the treatment of RA. These data suggest that the cell structure or function and signal transducing processes are the major processes during the treatment of ISL or RA, and that their overrepresentation may be due to the differentiation of melanoma cells.

3.7. Pathway analysis of DEGs during the treatment of ISL or RA

To identify the biological pathways that are active in ISL or RA treated B16F0 cells, we mapped the detected genes to reference canonical

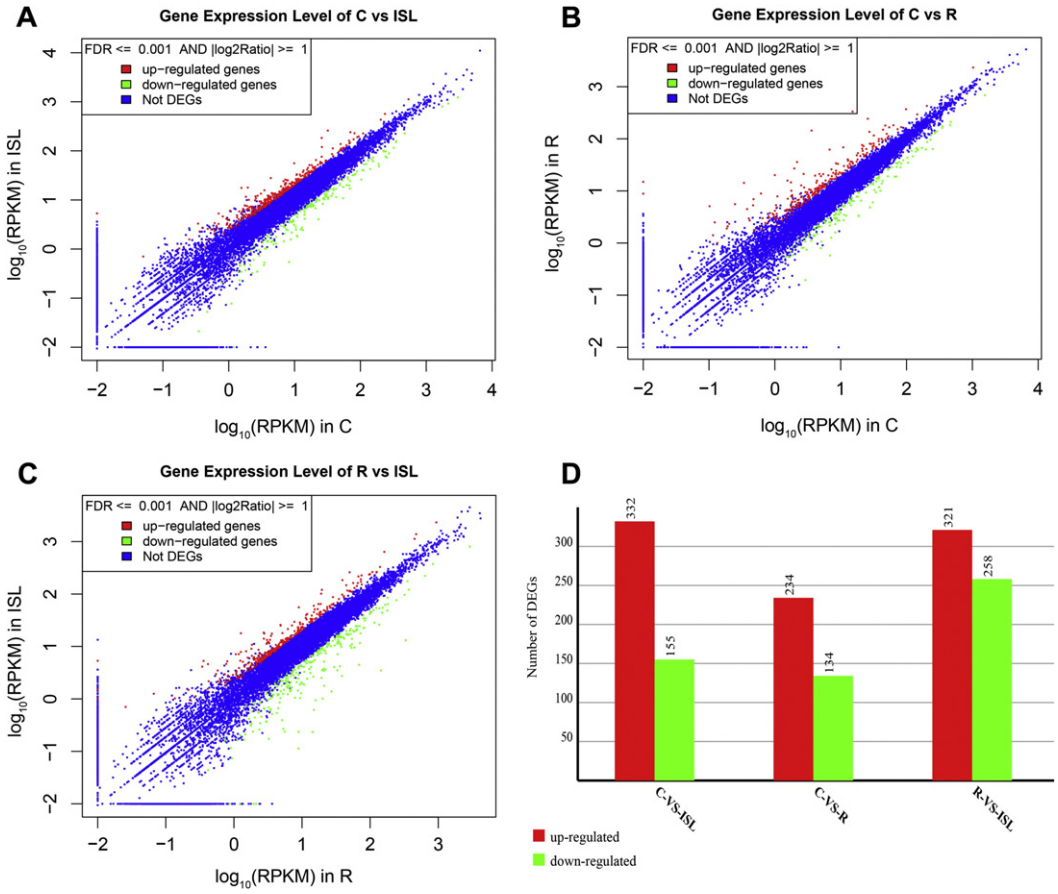

Fig. 2. Expression level and statistics of the differentially expressed genes (DEGs) between samples. (A) Expression level of DEGs in C-vs-ISL. (B) Expression level of DEGs in C-vs-RA. (C) Expression level of DEG in RA-vs-ISL. (D) Changes in gene expression profile among C, ISL, RA. The number of up-regulated and down-regulated genes in C-VS-ISL, C-VS-RA and RA-VS-ISL are summarized. Between the C and ISL libraries, there are 332 genes up-regulated and 155 genes down-regulated, while there are 234 up-regulated genes and 134 down-regulated genes between the C and RA libraries.

pathways in the Kyoto Encyclopedia of Genes and Genomes (KEGG) (http://www.genome.ad.jp/kegg/) (Park et al., 2008) (Fig. 6). Of the total 16,857 genes with pathway annotation, 390 and 304 were assigned to 201 and 193 KEGG pathways with the treatment of ISL and RA respectively. Those pathways with the greatest representation by unique genes were for glutathione metabolism (13/390 DEGs); glycolysis/gluconeogenesis (13/390 DEGs); and pentose phosphate pathway (7/390 DEGs) during the treatment of ISL. And the majority of the differentially expressed genes were found to be associated with MAPK signaling pathway (23/304 DEGs), carbohydrate digestion and

Table 2
Top 10 upregulated and downregulated genes after ISL treatment.

Symbol	Description	Gene ID	Fold change	*p*-Value	FDR
Up-regulated					
Gsta3	Glutathione S-transferase, alpha 3	14859	533.35	7.56E−12	1.36E−10
Spta1	Spectrin alpha, erythrocytic 1	20739	13.96	4.17E−07	3.88E−06
Gdf15	Growth differentiation factor 15	23886	11.31	2.62E−19	8.41E−18
Lipt2	Lipoyl(octanoyl) transferase 2 (putative)	67164	9.63	9.46E−05	5.26E−04
Slc7a11	Solute carrier family 7 (cationic amino acid transporter, y + system), member 11	26570	9.17	1.75E−143	5.20E−141
Blvrb	Biliverdin reductase B (flavin reductase (NADPH))	233016	8.11	2.97E−184	1.23E−181
A530050N04Rik	RIKEN cDNA A530050N04 gene	442846	7.54	7.19E−09	8.82E−08
Srxn1	Sulfiredoxin 1 homolog (*S. cerevisiae*)	76650	7.12	0	0
Xaf1	XIAP associated factor 1	327959	6.74	1.41E−06	1.19E−05
Fbxo2	F-box protein 2	230904	6.41	7.13E−27	3.45E−25
Down-regulated					
Creb5	cAMP responsive element binding protein 5	231991	−117.72	1.10E−05	7.77E−05
Dsp	Desmoplakin	109620	−16.62	1.06E−04	5.84E−04
Stc1	Stanniocalcin 1	20855	−15.16	1.59E−33	1.01E−31
Synm	Synemin, intermediate filament protein	233335	−14.19	4.09E−10	6.00E−09
Col12a1	Collagen, type XII, alpha 1	12816	−9.00	5.30E−06	4.01E−05
Tet1	Tet methylcytosine dioxygenase 1	52463	−7.83	1.46E−32	9.10E−31
Gm13889	Predicted gene 13889	620695	−7.27	1.08E−04	5.92E−04
Apln	Apelin	30878	−7.06	7.73E−07	6.85E−06
Fyb	FYN binding protein	23880	−6.53	3.34E−08	3.70E−07
Cacna1a	Calcium channel, voltage-dependent, P/Q type, alpha 1A subunit	12286	−6.35	8.26E−10	1.16E−08

Table 3
Top 10 upregulated and downregulated genes after RA treatment.

Symbol	Description	Gene ID	Fold change	*p*-Value	FDR
Up-regulated					
Fcna	Ficolin A	14133	1492.44	1.49E−28	8.17E−27
Efhd1	EF hand domain containing 1	98363	885.51	2.34E−23	1.07E−21
Plekhb1	Pleckstrin homology domain containing, family B (evectins) member 1	27276	50.07	2.71E−14	7.63E−13
Vdr	Vitamin D receptor	22337	42.04	2.76E−77	4.26E−75
Akap12	A kinase (PRKA) anchor protein (gravin) 12	83397	39.87	0	0
Lcn2	Lipocalin 2	16819	22.48	2.34E−06	2.69E−05
Dhrs3	Dehydrogenase/reductase (SDR family) member 3	20148	22.00	0	0
Ppm1j	Protein phosphatase 1J	71887	20.44	8.82E−06	9.02E−05
Lif	Leukemia inhibitory factor	16878	20.11	1.19E−88	2.18E−86
Tmem141	Transmembrane protein 141	51875	16.54	4.74E−41	3.56E−39
Down-regulated					
Ptgir	Prostaglandin I receptor (IP)	19222	−15.01	5.96E−11	1.28E−09
Cyp4b1	Cytochrome P450, family 4, subfamily b, polypeptide 1	13120	−11.94	2.62E−13	6.90E−12
Sgcg	Sarcoglycan, gamma (dystrophin-associated glycoprotein)	24053	−6.25	1.49E−13	3.98E−12
Mgll	Monoglyceride lipase	23945	−5.81	4.80E−75	7.01E−73
Gsta2	Glutathione S-transferase, alpha 2 (Yc2)	14858	−5.68	2.93E−05	2.68E−04
Ano3	Anoctamin 3	228432	−5.67	1.35E−74	1.95E−72
Cav1	Caveolin 1, caveolae protein	12389	−5.61	1.48E−33	9.28E−32
Dusp2	Dual specificity phosphatase 2	13537	−5.22	1.05E−09	2.03E−08
Ahnak	AHNAK nucleoprotein (desmoyokin)	66395	−5.08	0	0
Synm	Synemin, intermediate filament protein	233335	−5.02	1.68E−06	1.99E−05

absorption (7/304 DEGs), and amoebiasis (12/304 DEGs) with the treatment of RA.

4. Discussion

In this study, we have applied high-throughput single-end sequencing of cDNA (RNA-seq) as a systematic means to investigate the gene expression profiles in ISL/RA treated with or without melanoma cells. We identified 487 and 368 DEGs for the ISL and RA treatment including previously uninvestigated molecules. A pathway analysis of these DEGs revealed that the most significant biofunction in ISL treatment was the "glutathione metabolism", and "MAPK signaling pathway" by in RA treatment. We also found that the glycolysis/gluconeogenesis pathway and Pentose phosphate pathway and other sets of metabolic pathway-related genes were significantly down-regulated by ISL. These results point to the critical role that anti-oxidative defense and glycometabolism in the B16 mouse melanoma cell differentiation induced by ISL, and MAPK signaling in the RA treatment. This finding facilitates the understanding of melanoma differentiation process and leads a way for new drug discovery.

To our knowledge, this is the first reported study of extensive changes in gene expression of ISL-treated melanoma cells. Although another study have examined the gene expression treated by RA using microarray (Estler et al., 2008), the molecular mechanisms remain unclear. In contrast to RNA-seq, expression microarrays have a number of limitations (e.g., reliance on existing knowledge about the genome sequence, background noise and lower dynamic range). We therefore performed RNA-seq to generate a global view of drug induced differentiation of melanoma. Comparison of the identity of RA-regulated genes by RNA-seq in this study reported here reveals some commonality of genes such as akap12, ATPase, Ltbp1, Prkca, Anpep and zinc finger protein, but also a number of different gene expression changes. Possible explanations for these differences are analysis of different technology to detect, and different method of statistical analysis.

By focusing on only those genes which significantly >10 fold increased or decreased in samples a list of common 'top hits' was created (Tables 2 and 3). We discovered novel 7 genes (3 up-regulated, 4 down-regulated) altered after the ISL treatment, and 22 genes (20 up-regulated, 2 down-regulated) in the RA treatment. There was a major increase in the number of genes which expression changed at 48 h of compounds treatment that were up-regulated outnumbered those that were down-regulated. When genes were ranked by fold-change (FC), Gsta3 (a member of a group of zinc-finger transcription factors) involved in cell development and differentiation was one of the most up-regulated genes overall with a 533.35-fold increase treated after ISL treatment. Li Y et al. found Gsta3 played an important role in the prevention of bladder cancer progression and metastasis by inhibiting cell migration and invasion (Li et al., 2014). Moreover, it has been suggested decreased expression of Gsta3 accompanied with increasing tumor grade in breast cancer (Thewes et al., 2010). The increasing expression of Gsta3 in our data demonstrated melanoma cells revealed a grade malignancy reduction characteristic. Jowsey IR et al. have identified Gsta3 as a novel adipocyte differentiation-associated protein (Jowsey et al., 2003a). Previous studies also showed transcription factor Gsta3 was essential for differentiation of both Th2 cells and Ilc2 (KleinJan et al., 2014) and had potential value in differentiating small cell carcinomas of prostate origin from those of bladder origin (Bezerra et al., 2014). Gsta3 also played a role in the regulation of proliferation and/or differentiation processes in human primary keratinocytes (Masse et al., 2014). Furthermore, it has been reported Gsta3 as a direct target for Notch signaling is a critical element determining inductive Th2 differentiation and limiting Th1 differentiation (Amsen et al., 2007). Growth differentiation factor 15 (Gdf15), a member of the transforming growth factor-beta (TGF-beta) super-family, was also up-regulated by ISL. Ichikawa T et al. found TAp63-dependent induction of growth differentiation factor 15 (Gdf15) plays a critical role in the regulation of keratinocyte differentiation (Ichikawa et al., 2008). Our finding indicated that Gsta3 and Gdf15 may therefore be useful markers for evaluating ISL induced differentiation of melanoma.

Significant expression change of genes are found in the RA-treatment. Although, highly expressed gene Fcna and Plekhb1 which fold-change is 1492.44 and 50.07 respectively, had no function been ascribed to its predicted protein. Efhd1, which FC is 885.51, was mentioned in the research of fraternal twins. Dutting S et al. found Swiprosin-1/Efhd2. Swiprosin-2/Efhd1, two homologous EF-hand containing calcium binding adaptor proteins, modulates apoptosis and differentiation of neuronal and muscle precursor cells and swiprosin-2/Efhd1 is part of a cellular response to oxidative stress (Dütting et al., 2011). It has been reported that VDR expressed in cutaneous melanomas as marker of tumor progression (Kosiniak-Kamysz et al., 2014). High VDR expression determines a less malignant phenotype and relates to better prognosis for the progression of the disease. Akap12, Rarb and Pmepa1 are genes with tumor suppressor properties (Flotho et al., 2007; Yoon et al., 2007; Moison et al., 2014; Li & Li, 2015; Xu

et al., 2003), which also were up-regulated by RA treatment. We also found the increased expression of Dhrs3. Likewise there are numerous reports that RA alters the expression of Rarb and Dhrs3 which have functions in the bioactive of all trans retinoic acid. Retinoic acid receptor, beta (Rarb) is one of the three subtypes of retinoic acid receptors (PAR), which binds RA (Benbrook et al., 1988). The retinoic acid inducible dehydrogenase reductase 3 (Dhrs3) is thought to function as a retinaldehyde reductase that controls the levels of all trans retinaldehyde, the immediate precursor for bioactive all trans retinoic acid (Adams et al., 2014). Moreover, there are a variety of studies showing Lif, Lgi4, Pmepa1 and Gfra1 involve in the cell differentiation process with a FC ≥ 10 enhanced. Sun L et al. found leukemia inhibitory factor (LIF) playing divergent roles in different cell types: induces differentiation in preadipocytes and, however, inhibits differentiation in pluripotent murine embryonic stem (mES) cells (Sun et al., 2007). Lgi4 could promote the proliferation and differentiation of glial lineage cells throughout the developing peripheral nervous system (Nishino et al., 2010). Pmepa1 was thought to be a transforming growth factor-beta-induced marker of terminal colonocyte differentiation (Brunschwig et al., 2003). He Z et al. discovered Gfra1 silencing in mouse spermatogonial stem cells results in their differentiation via the inactivation of RET tyrosine kinase (He et al., 2007). However, no evidence and function research has been published that RA regulates Plekhb1, Ppm1j, Tmem141 and Gstm7 which were up-regulated in our data. The increasing expression of differentiation-related genes may give us a deep recognition of the mechanism of RA-induced melanoma differentiation by RNA-seq and make up the shortage of microarray at the same time.

The possible functions of the assembled DGEs were analyzed through their matching to the KEGG database, and the results indicated that the largest number of DEGs were included in glutathione metabolism, glycolysis/gluconeogenesis and pentose phosphate pathway (top three pathway that DGEs significantly enrich) treated after ISL. This finding indicates that anti-oxidative defense and glycometabolism is critical process in the ISL-induced melanoma differentiation. This finding is a complement to our previous research. In the current study, we found that the anti-oxidative response-related genes Gsta3 and Gclm were significantly up-regulated in glutathione metabolism treated after ISL. Glutathione S-transferase A3 (Gsta3), belonging to the alpha class glutathione S-transferases, are highly related and encode enzymes with glutathione peroxidase activity. The peroxidase activity associated with the GSTs is referred to as NonSe-GPX activity, which represents one of the important antioxidant mechanisms that exist in cells for protection against hydroperoxides, classified as reactive oxygen species (ROS) (Prohaska & Ganther, 1977). The significant increasing expression change by ISL indicated a cellular anti-oxidation adaptation process. In addition, the dramatic expression profile of Gsta3 observed in our RNA-seq data during ISL-induced melanoma differentiation also raises important questions as to how the Gsta3 gene is regulated. Previous study showed that Nrf2 regulates Gsta3 gene expression in a number of mouse tissues (Jowsey et al., 2003b). Further studies are still needed for the detailed explanation of the regulation of Nrf2 on Gsta3. The rate-limiting enzyme in GSH synthesis is glutamate cysteine ligase and polymorphisms in its catalytic and modifier subunits (Gclc and Gclm) have been shown for compromised response to oxidative stress amenable to in vitro and in vivo investigations (Schrottmaier, 2014; Cole et al., 2011). Harris and colleagues assessed the effects of genetic deletion of glutamate-cysteine ligase, modifier subunit (Gclm), which mediates GSH synthesis, impaired tumor initiation and progression in several mouse models of spontaneous tumor development and they also found deficiency in Gclm led to a 75% decrease in GSH levels, shifting the cells to a state of chronic oxidant stress (Harris et al., 2015). Consistent with this idea, Gclm-deficient cells exhibited increased expression of the antioxidant transcription factor nuclear factor (erythroid-derived 2)-like factor 2 (Nfe2l2, also known as Nrf2), which may compensate for decreased GSH synthesis to facilitate cell survival. This work suggested Gclm with an antioxidant ability could play a major role in driving cancer progression and affect the phenotypic behavior of cancer cells, also prompt Nrf2 was one of upstream regulators simultaneously. Nrf2 is a potent transcriptional activator and plays an important role in cellular antioxidant defense. Nrf2 transcriptional targets include glutathione cysteine ligase (GCL), involved in the rate-limiting step of biosynthesis of antioxidant glutathione; glutathione-utilizing enzymes such as glutathione S-transferase (GST); and haeme oxigenase 1 (HMOX1), involved in the catabolism of pro-oxidant haeme (Jung & Kwak, 2013). The current paradigm of Nrf2 regulation has mainly focused on oxidative stress-induced post-translational mechanisms, including regulation by its negative regulators (Keap1, Bach1, and b-TrCP), positive regulators (DJ1, p62, and p21), or protein modifications (Chowdhry et al., 2013). Our profiling results of increasing expression of Gata3 and Gclm, target of Nrf2, may implicate Nrf2 displays a potentially role in the melanoma differentiation mechanism induced by ISL. We also found several known anti-oxidant enzymes (Gstm6, Gsr, Gpx4, Gclc, Gstm1, G6pdx, Mgst1, Odc1) were elevated in glutathione metabolism as a correlate to the ISL treatment (Table S7). Based upon the gene expression profiles, we can conjecture a shift of the cellular redox state towards a strongly changed cellular milieu.

Glycolysis is regulated by slowing down or speeding up certain steps in the glycolysis pathway. This is accomplished by inhibiting or activating the enzymes that are involved. The three regulated enzymes are hexokinase (HK), phosphofructokinase (PFK-1), and pyruvate kinase (PK). Our results showed the down-regulation of hexokinase 2 (HK2), phosphofructokinase (PFK-1) and other enzymes like enolase 1B (Eno1b), phosphofructokinase (Pfkp), triosephosphate isomerase 1 (Tpi1), lactate dehydrogenase A (Ldha), phosphoglucomutase 2 (Pgm2), glucose phosphate isomerase 1 (Gpi1), aldehyde dehydrogenase 16 family, member A1 (Aldh16a1) are directly associated with a decrease in glycolysis treated after ISL. Furthermore, pseudogene 5069 (Gm5069) that have not been previously reported. Hexokinase 2 (HK2), coding for the first rate-limiting enzyme of glycolysis, has a critical role in cancer cells' proliferation among the top list of genes predicted. In highly proliferative cancer cells, the up-regulation of glycolysis in cancer cells (the “Warburg effect”) is common and has implications for prognosis and treatment. And the highly glycolytic phenotype is supported by hexokinase (primarily HK 2) that is over expressed and bound to the outer mitochondrial membrane via the porin-like protein voltage-dependent anion channel (VDAC). This protein and the adenine nucleotide transporter move ATP, newly synthesized by the inner membrane located ATP synthase, to active sites on HK 2. The abundant amounts of HK 2 bind both the ATP and the incoming glucose producing the product glucose-6-phosphate, also at an elevated rate. This critical metabolite then serves both as a biosynthetic precursor to support cell proliferation and as a precursor for lactic acid, the latter exiting cancer cells causing an unfavorable environment for normal cells. Phosphofructokinase is an important control point in the glycolytic pathway, since it is one of the irreversible steps and has key allosteric effectors, AMP and fructose 2,6-bisphosphate (F2,6BP). The decreased expression of Hexokinase 2 and phosphofructokinase suppress the “Warburg Effect” in cancer while helping prevent cell proliferation.

The pathophysiological status of solid malignant tumours is characterised by pronounced tissue acidosis and hypoxia (Semenza, 2011) and by enhanced formation and accumulation of lactate

Fig. 3. qPCR validation of RNA-seq data. Relative quantitation was carried out to measure changes target gene expression in samples relative to an endogenous reference sample. Results are expressed as the target/reference ratio of each sample normalized by the target/reference ratio of the calibrator. GAPDH was used as a reference gene. The vertical axis indicates the fold change of transcript abundance in ISL (Fig. 4A) or RA (Fig. 4B) treated B16F0 cells compared to the control cells. (qPCR-P: the RNA samples from pooling samples that were used for deep sequencing; qPCR-B: the RNA samples from independent RNA extractions from biological replicates).

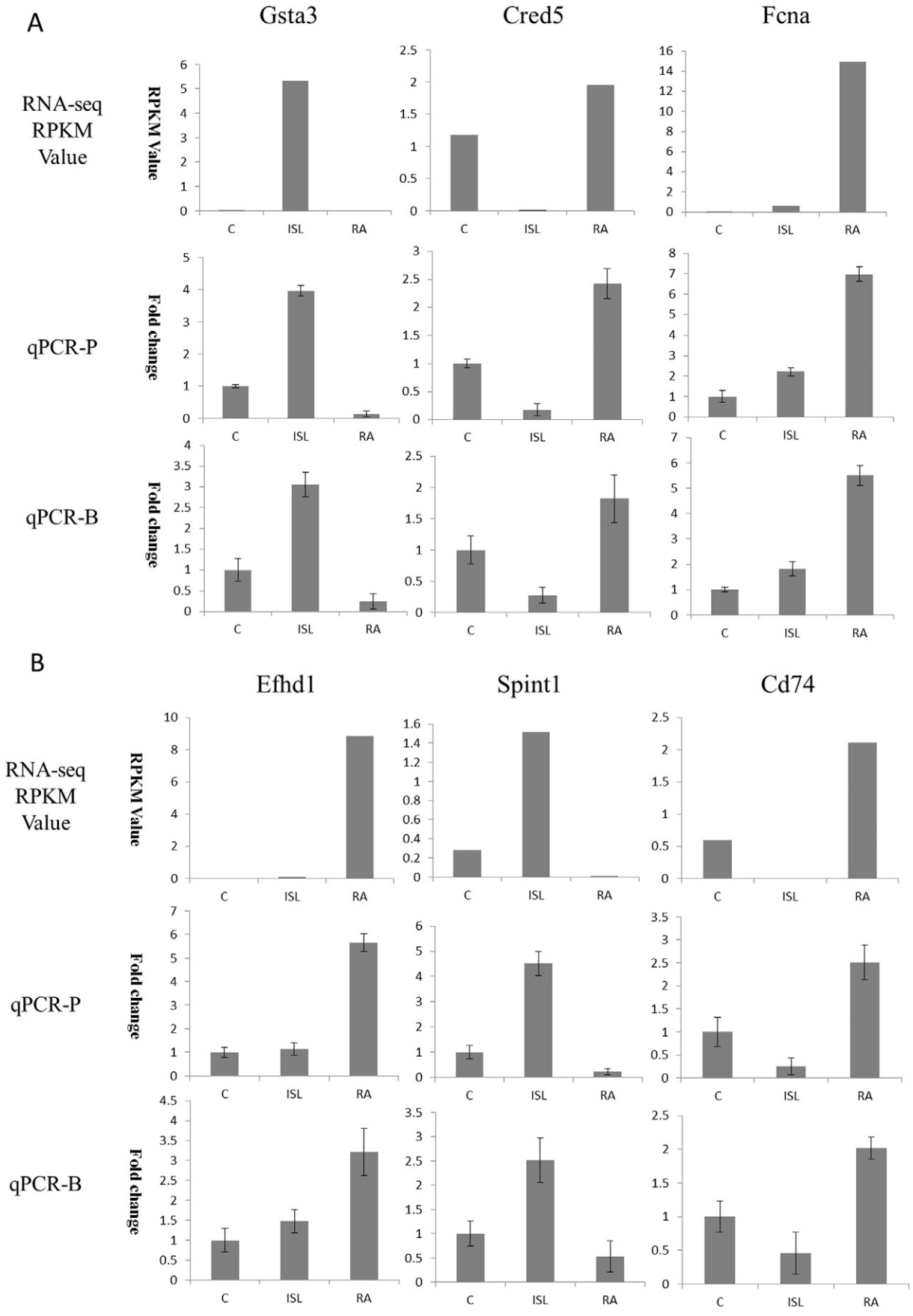
A
Gsta3
Cred5
Fcna
RNA-seq RPKM Value
qPCR-P
qPCR-B
RPKM Value
Fold change
C
ISL
RA
B
Efhd1
Spint1
Cd74

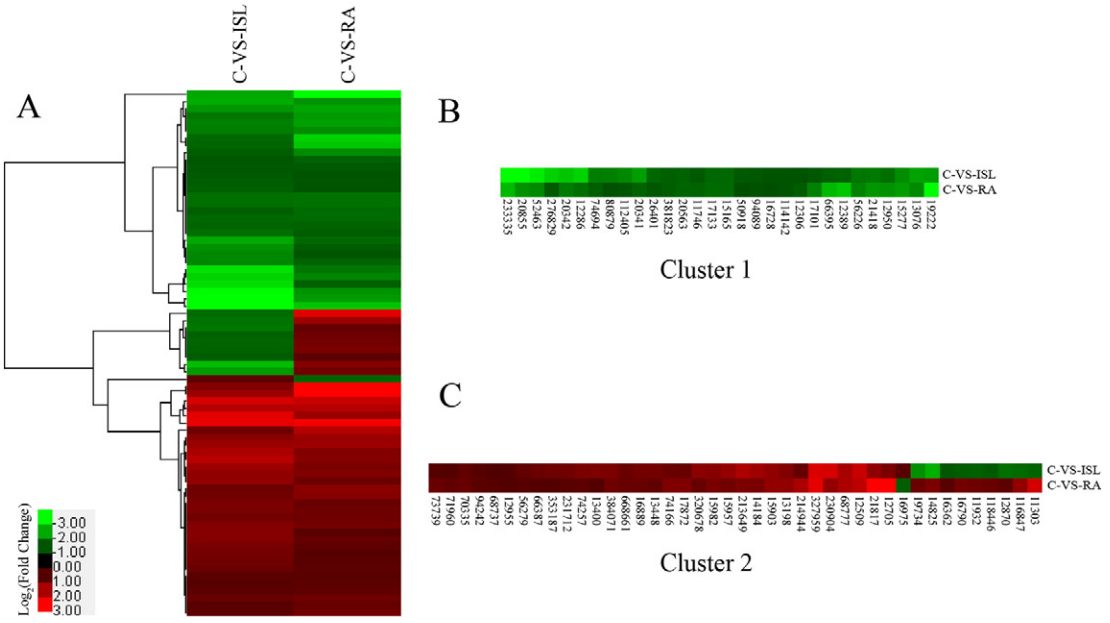

Fig. 4. Hierarchical cluster analysis of gene expression based on log ratio RPKM data. The colour means Log2(Fold-change) of the differential expression profiles. Green represents lower expression, red represents high expression, columns represent individual experiments, and rows represent transcriptional units. Two-dimensional hierarchical clustering classifies 72 differential expression profiles into two expression cluster groups according to the similarity of their expression profiles. Their identities and expression patterns are listed in Tables S1 and S2.

(Walenta et al., 2004; Walenta & Mueller-Klieser, 2004). The latter property is mainly due to an increase in glycolytic flux which is caused by up-regulated expression and, in parts, by biochemical activation of membrane-based transporters for glucose and monocarboxylates and of glycolytic enzymes as a consequence of metabolic and oncogenic regulation (Koukourakis et al., 2006). Hypoxia can shift the balance of energy production towards anaerobic glycolysis with production of lactate, but many tumours exhibit a strong generation of lactate even in the presence of oxygen. This phenomenon which is known as 'aerobic glycolysis' or the 'Warburg effect' is generally considered to be the result of oncogenic alteration in glucose metabolism following malignant transformation (Kroemer & Pouyssegur, 2008). The concomitant induction of angiogenesis and glycolysis with cell proliferation is mediated

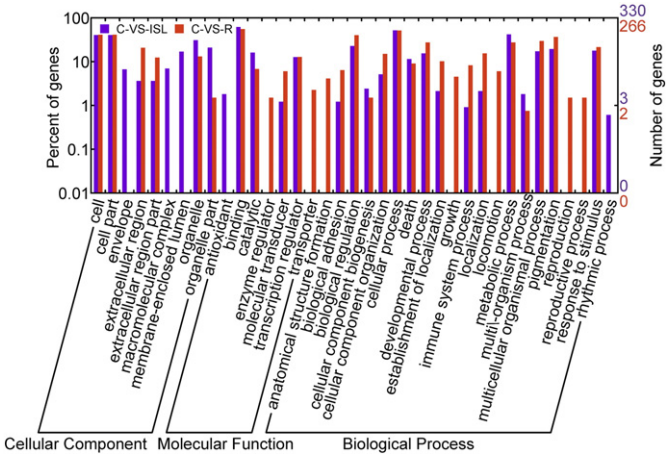

Fig. 5. Histogram presentation of Gene Ontology (GO) classification. The results are summarized in three main categories: biological process, molecular function and cellular component. The y-axis indicates the number of genes in a category. In three main categories of GO classification, there are 27, 10 and 12 functional groups in ISL treatment and 27, 10, and 11 functional groups in RA treatment, respectively. Among these groups, the GO terms binding (GO: 0005488) in the molecular function categories and response to stimulus in the biological process categories (GO: 0050896) were both dominant in the treatment both of ISL and RA.

partly by activating hypoxia-inducible transcriptional factor (HIF-1). Hypoxia increases HIF-1 levels in most cell types and HIF-1 mediates adaptative responses to changes in tissue oxygenation. Thus, HIF-1 can directly up-regulate expression of a set of genes involved in both local and global reaction to hypoxia, including angiogenesis, erythropoiesis, breathing and most of the glycolytic enzymes: HK1, HK2, AMF/GPI, ENO1, GLUT1, GADPH, LDHA, PFKBF3, PFKL, PGK1, PKM, TPI (Semenza, 1998). These data support a functional link between enhanced glycolysis and cellular oxidative stress adaptation during tumor formation and expansion. ROS (reactive oxygen species) is the main source of oxidative stress. Normal levels of cellular ROS can work as second messengers involved in several signal transduction pathways (such as the Ras-Raf-MEK cascade) (Dang, 2007). But abnormal ROS accumulation and its side-effects over intracellular macromolecules (oxidation of lipid, protein and DNA) provokes cumulative damage at cell, tissue, and organism level, and even cause tumor differentiation (Chen et al., 2012). Our previous result revealed that the ROS level increased during melanoma differentiation induced by ISL. Increased ROS accumulation may disturb the hypoxia environment for melanoma including causing ROS-mediated fixation of DNA damage and induction of radio resistance. In our RNA-seq data, glutathione metabolism-related genes were up-regulated and glycolysis-related genes were down-regulated. This finding may be connected with the key molecular HIF-1. HIF-1 transcriptionally regulates most of glycolytic genes with the only exception of PGM (Niizeki et al., 2002). It suggested that ISL-induced ROS increase may decrease the expression of HIF-1 while resulting in a reduction of HK 2 expression to adapt high ROS state. Meanwhile, Glutathione (GSH: reduced glutathione; GSSG: oxidised glutathione) which is quantitatively the most important cellular redox system was also increased by ISL to induce a reduced milieu for melanoma. The pentose phosphate pathway (PPP), i.e., the activity of glucose-6-phosphate dehydrogenase, plays a prominent role to continuously yield NADPH + H^+ to keep glutathione in the reduced state. The three vital metabolism pathways which DGEs significantly enrich may probably provide insights into the molecular mechanisms of the melanoma differentiation induced by ISL.

Our data set also allow us to identify pathway in RA-induced melanoma differentiation. The KEGG analysis indicated that the most of

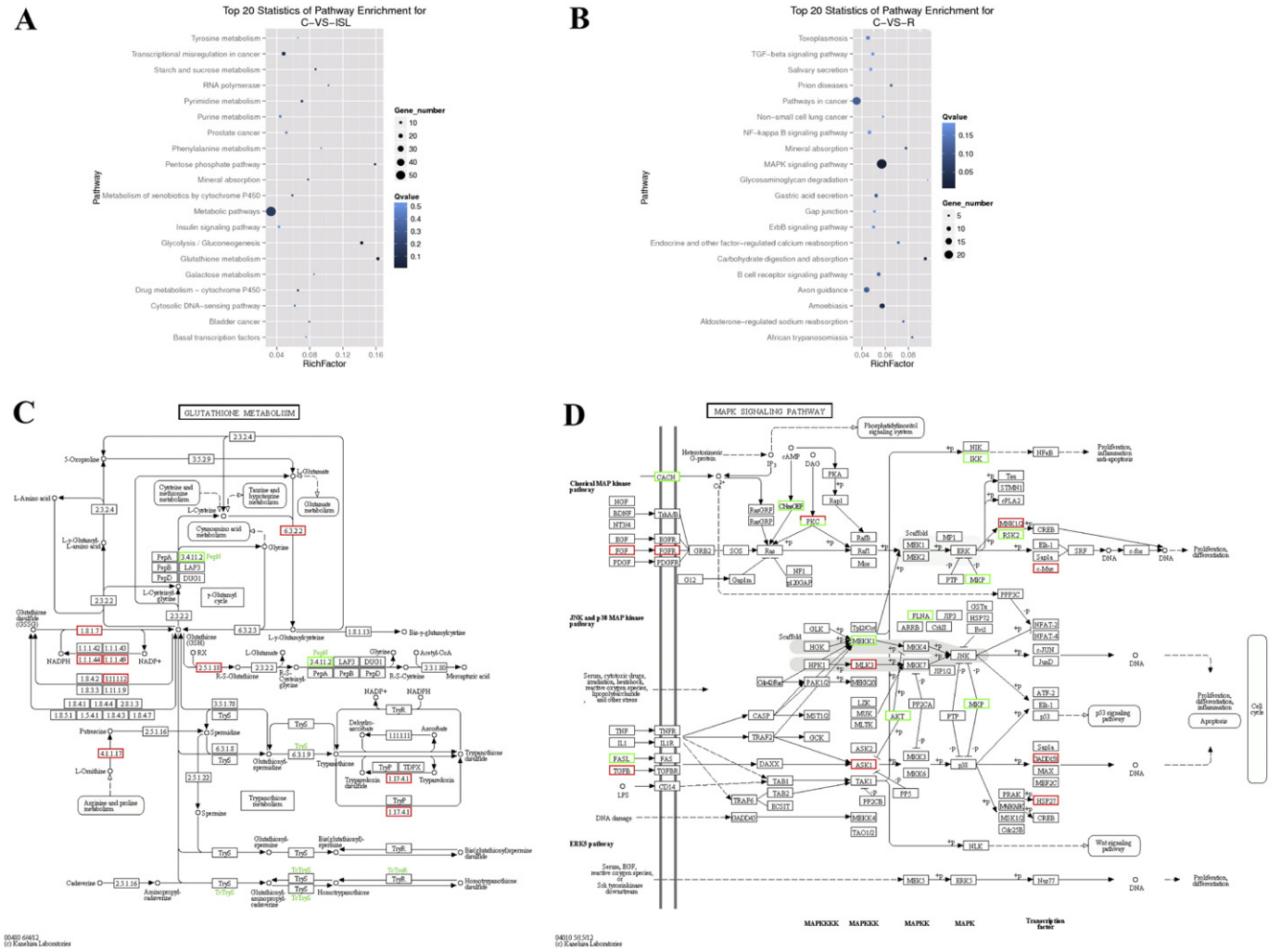

Fig. 6. Scatter plot of KEGG pathway enrichment statistics and the most enrichment pathway during the treatment of ISL or RA. (A) Top 20 statistics of pathway enrichment after ISL treatment. (B) Top 20 statistics of pathway enrichment after RA treatment. (C) Glutathione metabolism signaling pathway (D) MAPK signaling pathway. Red and green frames indicate genes and enriched functions that were up- and down-regulated in drug treatment.

annotated DGEs were enriched in MAPK signaling pathway. Mitogen-activated protein kinases (MAPKs) are serine-threonine kinases that mediate intracellular signaling associated with a variety of cellular activities including cell proliferation, differentiation, survival, death, and transformation (McCubrey et al., 2007; Dhillon et al., 2007). Interestingly, previous work had found many different MAPKs cascades can be activated following ROS accumulation. These include the ROS-responsive MAPKKK MEKK1, MPK4 and MPK6 (Jammes et al., 2009). MAPK pathways are also implicated in the induction of nitric oxide (NO) and ROS bursts and signaling, which synergistically function in defense responses (Asai et al., 2008). Both NO and ROS were reported to be produced simultaneously through the MAPK cascade MEK2-SIPK (salicylic acid-induced protein kinase) (Demidchik et al., 2009). Except for the findings as previously reported, we also predicted several potential genes in MAPK signaling pathway. This finding provides a good foundation for further research on the discovery of new genes and facilitates the understanding of RA induced melanoma differentiation.

There have been a number of earlier reports of differentiation related gene. Here, we apply ISL or RA induced melanoma differentiation to predict melanoma related differentiation gene. In the analysis of hierarchical clustering of DEGs, we discover 72 DEGs. In 72 DEGs, there were 32 DEGs up-regulated, and 30 DEGs down-regulated in both ISL and RA treatment. Among these genes, we found Cited1, Tgm2, Xaf1, Cd59a, Fbxo2, Adh7 were highly expressed in both ISL and RA treatment. We suggested an important role on melanoma differentiation of these genes. Xaf1 was expressed in top 10 within ISL treatment and top 30 after treated by RA. Cited1 is a non-DNA binding transcriptional co-regulator whose expression can distinguish the 'proliferative' from 'invasive' signature in the phenotype-switching model of melanoma. It is reported Cited1 positively correlates with Mitf expression and can discriminate the MITF-high/pigmentation tumor molecular subtype in a large cohort (120) of melanoma cell lines (Howlin et al., 2015). Besides, Mitf functioned in a range compatible with tumourigenesis. So, we could speculate B16F0 melanoma showed a high pigmentation ability and a loss malignant characterization after both ISL and RA. Furthermore, Yang D et al. found Cited1 modulates parathyroid hormone regulation of osteoblastic differentiation (Yang et al., 2008). Plisov S et al. thought Cited1 may coordinate cellular differentiation and survival signals that regulate nephronic patterning in the metanephros (Plisov et al., 2005). These reports indicated Cited1 may contribute to the differentiation of melanoma. Previously, there were studies had reported TGM2 and ADH7 are involved in retinoic acid-induced transdifferentiation (Obinata et al., 2011). Previous study also suggests that TGM2 is useful as a predictive marker for patient prognosis and may be a novel therapeutic target for colorectal cancer and breast cancer (Miyoshi et al., 2010; Ai et al., 2008). This is the first report to show TGM2 and ADH7 highly expressed in ISL induced melanoma differentiation. We suggested these genes may have important functions in melanoma differentiation.

A limitation of our dataset in analyzing the melanoma differentiation event is that we only use melanoma cell lines and differentiation inducer treated melanoma cell lines. For limited experimental condition, our group of experiment lack of homologous melanocyte melan-a cell line as normal control. For sequencing method, we applied the single-end sequencing. Although this approach could be highly sensitive, it also results in high false positive rate. Further work using longer sequencing reads or using paired-end sequencing will help to alleviate the problem.

In conclusion, this study for the first time utilized next generation sequencing platform to comprehensively characterize the process of melanoma differentiation. The full characterize of the landscapes of melanoma transcriptome provides the basis for an understanding of the molecular mechanism of compound induced melanoma differentiation. Future research works based on our findings may speed up the discovery of novel biomarkers and drug targets for improving diagnosis and therapy of melanoma.

5. Conclusion

Melanoma represents a significant and growing public health burden worldwide. Our previous evidence clearly demonstrates that ISL could induce melanoma cell line B16F0 differentiation which provide a new way to cue melanoma. Then, we deeply dig the mechanisms of ISL-induced B16F0 differentiation by next generation sequencing (NGS). Interesting findings showed in our research: anti-oxidative defense and glycometabolism are critical process in the ISL-induced melanoma differentiation. These findings provide a molecular basis for ISL-induced melanoma differentiation process. This investigation has also provided insight into the mechanism of melanoma differentiation in RA treatment. After the interference of RA, DEGs reveals in MAPK signaling pathway. It seems that the pattern of ISL and RA induced melanoma differentiation is quite different. We also detects 72 DEGs which probably related to melanoma differentiation. Our future research based on these findings may speed up the discovery of novel biomarkers of melanoma differentiation and drug targets for improving diagnosis and therapy of melanoma.

Supplementary data to this article can be found online at http://dx.doi.org/10.1016/j.gene.2016.07.052.

Conflict of interest

There has no conflict of interest.

Acknowledgements

This study was supported by the National Natural Science Foundation of China (No. 31471338), and fund of Binzhou Medical University (BY2014KYQD01), the Xinjiang Production and Construction Corps Funds for innovation team in key areas (2015BD005) to Q.S. Zheng.

References

Adams, M.K., Belyaeva, O.V., Wu, L., Kedishvili, N.Y., 2014. The retinaldehyde reductase activity of DHRS3 is reciprocally activated by retinol dehydrogenase 10 to control retinoid homeostasis. J. Biol. Chem 289 (21), 14868–14880 May 23.

Ai, L., Kim, W.J., Demircan, B., Dyer, L.M., Bray, K.J., Skehan, R.R., Massoll, N.A., Brown, K.D., 2008. The transglutaminase 2 gene (TGM2), a potential molecular marker for chemotherapeutic drug sensitivity, is epigenetically silenced in breast cancer. Carcinogenesis 29 (3), 510–518 Mar.

Alesiani, D., Cicconi, R., Mattei, M., Montesano, C., Bei, R., Canini, A., 2008. Cell cycle arrest and differentiation induction by 5,7-dimethoxycoumarin in melanoma cell lines. Int. J. Oncol 32 (2), 425–434 Feb.

Amin, A., Buratovich, M., 2007. The anti-cancer charm of flavonoids: a cup-of-tea will do! Recent Pat. Anticancer Drug Discov 2 (2), 109–117 Jun.

Amsen, D., Antov, A., Jankovic, D., Sher, A., Radtke, F., Souabni, A., Busslinger, M., McCright, B., Gridley, T., Flavell, R.A., 2007. Direct regulation of Gata3 expression determines the T helper differentiation potential of Notch. Immunity 27 (1), 89–99 Jul.

Asai, S., Ohta, K., Yoshioka, H., 2008. MAPK signaling regulates nitric oxide and NADPH oxidase-dependent oxidative bursts in *Nicotiana benthamiana*. Plant Cell 20 (5), 1390–1406 May.

Atkinson, J.M., Rank, K.B., Zeng, Y., Capen, A., Yadav, V., 2015. Manro JR et al. activating the Wnt/β-catenin pathway for the treatment of melanoma–application of LY2090314, a novel selective inhibitor of glycogen synthase kinase-3. PLoS One 10 (4) Apr 27.

Audic, S., Claverie, J.M., 1997. The significance of digital gene expression profiles. Genome Res 7 (10), 986–995 Oct.

Bajetta, E., Del Vecchio, M., Bernard-Marty, C., Vitali, M., Buzzoni, R., 2002. Olivier Rixe. Semin. Oncol 29 (5), 427–445 October.

Barres B, Dugas J, Cell Cycle Regulation and Differentiation. WO2008013918, (2008).

Beddingfield III, F.C., 2003. The melanoma epidemic: resipsa loquitur. Oncologist 8 (5), 459–465.

Benbrook, D., Lernhardt, E., Pfahl, M., 1988. A new retinoic acid receptor identified from a hepatocellular carcinoma. Nature 333 (6174), 669–672 Jun 16.

Benjamini, Y., Yekutieli, D., 2001. The control of the false discovery rate in multiple testing under dependency. Ann. Stat 29, 1165–1188.

Bezerra, S.M., Lotan, T.L., Faraj, S.F., Karram, S., Sharma, R., Schoenberg, M., et al., 2014. GATA3 expression in small cell carcinoma of bladder and prostate and its potential role in determining primary tumor origin. Hum. Pathol 45 (8), 1682–1687 Aug.

Brunschwig, E.B., Wilson, K., Mack, D., Dawson, D., Lawrence, E., Willson, J.K., Lu, S., Nosrati, A., Rerko, R.M., Swinler, S., Beard, L., Lutterbaugh, J.D., Willis, J., Platzer, P., Markowitz, S., 2003. PMEPA1, a transforming growth factor-beta-induced marker of terminal colonocyte differentiation whose expression is maintained in primary and metastatic colon cancer. Cancer Res 63 (7), 1568–1575 Apr 1.

Buscà, R., Bertolotto, C., Ortonne, J.P., Ballotti, R., 1996. Inhibition of the phosphatidylinositol 3-kinase/p70 (S6)-kinase pathway induces B16 melanoma cell differentiation. J. Biol. Chem 271 (50), 31824–31830 Dec 13.

Cheli, Y., Giuliano, S., Botton, T., Rocchi, S., Hofman, V., Hofman, P., Bahadoran, P., Bertolotto, C., Ballotti, R., 2011. Mitf is the key molecular switch between mouse or human melanoma initiating cells and their differentiated progeny. Oncogene 30 (20), 2307–2318 May 19.

Chen, X., Zhang, B., Yuan, X., Yang, F., Liu, J., Zhao, H., et al., 2012. Isoliquiritigenin-induced differentiation in mouse melanoma B16F0 cell line. Oxidative Med. Cell. Longev 2012, 534934.

Chowdhry, S., Zhang, Y., McMahon, M., Sutherland, C., Cuadrado, A., Hayes, J.D., 2013. Nrf2 is controlled by two distinct β-TrCP recognition motifs in its Neh6 domain, one of which can be modulated by GSK-3 activity. Oncogene 32 (32), 3765–3781 Aug 8.

Chudnovsky, Y., Adams, A.E., Robbins, P.B., Lin, Q., Khavari, P.A., 2005. Use of human tissue to assess the oncogenic activity of melanoma-associated mutations. Nat. Genet 37 (7), 745–749 Jul Epub 2005 Jun 12.

Cole, T.B., Giordano, G., Co, A.L., Mohar, I., Kavanagh, T.J., Costa, L.G., 2011. Behavioral characterization of GCLM-knockout mice, a model for enhanced susceptibility to oxidative stress. J. Toxicol 2011, 157687.

Irani et al., 1997Dang, C.V., 2007. The interplay between MYC and HIF in the Warburg effect. In: Kroemer, G., Mumberg, D., Keun, H., Riefke, B., Steger-Hartmann, T., Petersen, K. (Eds.), Oncogenes Meet Metabolism, first ed. Springer, Berlin, Heidelberg, pp. 35–53.

de Hoon, M.J., Imoto, S., Nolan, J., Miyano, S., 2004. Open source clustering software. Bioinformatics 20 (9), 1453–1454 Jun 12.

Demidchik, V., Shang, Z., Shin, R., Thompson, E., Rubio, L., Laohavisit, A., Mortimer, J.C., Chivasa, S., Slabas, A.R., Glover, B.J., Schachtman, D.P., Shabala, S.N., Davies, J.M., 2009. Plant extracellular ATP signalling by plasma membrane NADPH oxidase and Ca^{2+} channels. Plant J 58 (6), 903–913 Jun.

Dhillon, A.S., Hagan, S., Rath, O., Kolch, W., 2007. MAP kinase signalling pathways in cancer. Oncogene 26 (22), 3279–3290 May 14.

Dütting, S., Brachs, S., Mielenz, D., 2011. Fraternal twins: Swiprosin-1/EFhd2 and Swiprosin-2/EFhd1, two homologous EF-hand containing calcium binding adaptor proteins with distinct functions. Cell Commun. Signal 9, 2 Jan 18.

Engan, T., Bjerve, K.S., Hoe, A.L., Krane, J., 1995. Characterization of plasma lipids in patients with malignant disease by 13C nuclear magnetic resonance spectroscopy and gas liquid chromatography. Blood 85 (5), 1323–1330 Mar 1.

Estler, M., Boskovic, G., Denvir, J., Miles, S., Primerano, D.A., Niles, R.M., 2008. Global analysis of gene expression changes during retinoic acid-induced growth arrest and differentiation of melanoma: comparison to differentially expressed genes in melanocytes vs melanoma. BMC Genomics 9, 478 Oct 11.

Facchetti, F., Monzani, E., La Porta, C.A., 2007. New perspectives in the treatment of melanoma: anti-angiogenic and anti-lymphangiogenic strategies. Recent Pat. Anticancer Drug Discov 2 (1), 73–78 Jan.

Fang, D., Hallman, J., Sangha, N., Kute, T.E., Hammarback, J.A., White, W.L., Setaluri, V., 2001. Expression of microtubule-associated protein 2 in benign and malignant melanocytes: implications for differentiation and progression of cutaneous melanoma. Am. J. Pathol 158 (6), 2107–2115 Jun.

Fang, D., Nguyen, T.K., Leishear, K., Finko, R., Kulp, A.N., Hotz, S., Van Belle, P.A., Xu, X., Elder, D.E., Herlyn, M., 2005. A tumorigenic subpopulation with stem cell properties in melanomas. Cancer Res 65 (20), 9328–9337 Oct 15.

Flotho, C., Paulun, A., Batz, C., Niemeyer, C.M., 2007. AKAP12, a gene with tumour suppressor properties, is a target of promoter DNA methylation in childhood myeloid malignancies. Br. J. Haematol 138 (5), 644–650 Sep.

Grichnik, J.M., Burch, J.A., Schulteis, R.D., Shan, S., Liu, J., Darrow, T.L., Vervaert, C.E., Seigler, H.F., 2006. Melanoma, a tumor based on a mutant stem cell? J. Invest. Dermatol 126 (1), 142–153 Jan.

Gupta, P.B., Kuperwasser, C., Brunet, J.P., Ramaswamy, S., Kuo, W.L., Gray, J.W., Naber, S.P., Weinberg, R.A., 2005. The melanocyte differentiation program predisposes to metastasis after neoplastic transformation. Nat. Genet 37 (10), 1047–1054 Oct Epub 2005 Sep 4.

Harris, I.S., Treloar, A.E., Inoue, S., Sasaki, M., Gorrini, C., Lee, K.C., et al., 2015. Glutathione and thioredoxin antioxidant pathways synergize to drive cancer initiation and progression. Cancer Cell 27 (2), 211–222 Feb 9.

Hata, K., Mukaiyama, T., Tsujimura, N., Sato, Y., Kosaka, Y., Sakamoto, K., Hori, K., 2006l. Differentiation-inducing activity of lupane triterpenes on a mouse melanoma cell line. Cytotechnology 52 (3), 151–158. http://dx.doi.org/10.1007/s10616-007-9069-0 Nov. Epub 2007 Apr 20.

He, Z., Jiang, J., Hofmann, M.C., Dym, M., 2007. Gfra1 silencing in mouse spermatogonial stem cells results in their differentiation via the inactivation of RET tyrosine kinase. Biol. Reprod 77 (4), 723–733 Oct.

Herlyn, M., Clark Jr., W.H., Mastrangelo, M.J., Guerry, D.P., Elder, D.E., LaRossa, D., et al., 1980. Specific immunoreactivity of hybridoma-secreted monoclonal anti-melanoma antibodies to cultured cells and freshly derived human cells. Cancer Res 40 (10), 3602–3609 Oct.

Herlyn, M., Thurin, J., Balaban, G., Bennicelli, J.L., Herlyn, D., Elder, D.E., et al., 1985. Characteristics of cultured human melanocytes isolated from different stages of tumor progression. Cancer Res 45 (11 Pt 2), 5670–5676 Nov.

Howlin, J., Cirenajwis, H., Lettiero, B., Staaf, J., Lauss, M., Saal, L., et al., 2015. Loss of CITED1, an MITF regulator, drives a phenotype switch in vitro and can predict clinical outcome in primary melanoma tumours. PeerJ 3, e788 Feb 26.

Huang da, W., Sherman, B.T., Lempicki, R.A., 2009. Systematic and integrative analysis of large gene lists using DAVID bioinformatics resources. Nat. Protoc 4 (1), 44–57.

Ichikawa, T., Suenaga, Y., Koda, T., Ozaki, T., Nakagawara, A., 2008. TAp63-dependent induction of growth differentiation factor 15 (GDF15) plays a critical role in the regulation ofkeratinocyte differentiation. Oncogene 27 (4), 409–420 Jan 17.

Jammes, F., Song, C., Shin, D., Munemasa, S., Takeda, K., Gu, D., Cho, D., Lee, S., Giordo, R., Sritubtim, S., Leonhardt, N., Ellis, B.E., Murata, Y., Kwak, J.M., 2009. MAP kinases MPK9 and MPK12 are preferentially expressed in guard cells and positively regulate ROS-mediated ABA signaling. Proc. Natl. Acad. Sci. U. S. A. 106 (48), 20520–20525 Dec 1.

Jowsey, I.R., Smith, S.A., Hayes, J.D., 2003a. Expression of the murine glutathione S-transferase alpha3 (GSTA3) subunit is markedly induced during adipocyte differentiation: activation of the GSTA3 gene promoter by the pro-adipogenic eicosanoid 15-deoxy-delta12,14-prostaglandin J2. Biochem. Biophys. Res. Commun 312 (4), 1226–1235 Dec 26.

Jowsey, I.R., Jiang, Q., Itoh, K., Yamamoto, M., Hayes, J.D., 2003b. Expression of the aflatoxin B1-8,9-epoxide-metabolizing murine glutathione S-transferase A3 subunit is regulated by the Nrf2 transcription factor through an antioxidant response element. Mol. Pharmacol 64 (5), 1018–1028 Nov.

Jung, K.A., Kwak, M.K., 2013. Enhanced 4-hydroxynonenal resistance in KEAP1 silenced human colon cancer cells. Oxidative Med. Cell. Longev 2013, 423965.

Kelsall, S.R., Mintz, B., 1998. Metastatic cutaneous melanoma promoted by ultraviolet radiation in mice with transgene-initiated low melanoma susceptibility. Cancer Res 58 (18), 4061–4065 Sep 15.

King, R., Googe, P.B., Weilbaecher, K.N., Mihm Jr., M.C., Fisher, D.E., 2001. Microphthalmia transcription factor expression in cutaneous benign, malignant melanocytic, and nonmelanocytic tumors. Am. J. Surg. Pathol 25 (1), 51–57 Jan.

KleinJan, A., Klein Wolterink, R.G., Levani, Y., de Bruijn, M.J., Hoogsteden, H.C., van Nimwegen, M., Hendriks, R.W., 2014. Enforced expression of Gata3 in T cells and group 2 innate lymphoid cells increases susceptibility to allergic airway inflammation in mice. J. Immunol 192 (4), 1385–1394 Feb 15.

Kosiniak-Kamysz, A., Marczakiewicz-Lustig, A., Marcińska, M., Skowron, M., Wojas-Pelc, A., Pośpiech, E., Branicki, W., 2014. Increased risk of developing cutaneous malignant melanoma is associated with variation in pigmentation genes and VDR, and may involve epistatic effects. Melanoma Res 24 (4), 388–396 Aug.

Koukourakis, M.I., Pitiakoudis, M., Giatromanolaki, A., Tsarouha, A., Polychronidis, A., Sivridis, E., Simopoulos, C., 2006. Oxygen and glucose consumption in gastrointestinal adenocarcinomas: correlation with markers of hypoxia, acidity and anaerobic glycolysis. Cancer Sci 97, 1056–1060.

Kreider, J.W., Wade, D.R., Rosenthal, M., Densley, T., 1975a. Maturation and differentiation of B16 melanoma cells induced by theophylline treatment. J. Natl. Cancer Inst 54 (6), 1457–1467 Jun.

Kreider, J.W., Wade, D.R., Rosenthal, M., Densley, T., 1975b. Maturation and differentiation of B16 melanoma cells induced by theophylline treatment. J. Natl. Cancer Inst 54 (6), 1457–1467 Jun.

Krissansen GW, Kanwar JR, Ching L M, Cancer therapy. US2003003092, (2003).

Kroemer, G., Pouyssegur, J., 2008. Tumor cell metabolism: cancer's Achilles' heel. Cancer Cell 13 (6), 472–482 Jun.

Lens, M.B., Dawes, M., 2004. Global perspectives of contemporary epidemiological trends of cutaneous malignant melanoma. Br. J. Dermatol 150 (2), 179–185 Feb.

Li, H., Li, L., 2015. Relationship of GSTP1 lower expression and multidrug resistance reversing of curcumin on human colon carcinoma cells. Zhonghua Yi Xue Za Zhi 95 (30), 2478–2482 Aug 11.

Li, R., Yu, C., Li, Y., Lam, T.W., Yiu, S.M., Kristiansen, K., Wang, J., 2009. SOAP2: an improved ultrafast tool for short read alignment. Bioinformatics 25 (15), 1966–1967 Aug 1.

Li, Y., Ishiguro, H., Kawahara, T., Miyamoto, Y., Izumi, K., Miyamoto, H., 2014. GATA3 in the urinary bladder: suppression of neoplastic transformation and down-regulation by androgens. Am. J. Cancer Res 4 (5), 461–473 Sep 6.

Liu Y, Safe Natural Pharmaceutical Composition for Treating Cancer. US20040072790, (2004).

Liu, H.L., Jiang, W.B., Xie, M.X., 2010a. Flavonoids: recent advances as anticancer drugs. Recent Pat. Anticancer Drug Discov 5 (2), 152–164 Jun.

Liu T, Wang T, Cheng HM, Li DF, Guo L, Zhao WB, Wang ZH, Zheng QS, Temperature-controlled Sustained-Release Injection Containing Isoliquiritigenin and Preparation. CN101756888, (2010b).

Liu, J., Fukunaga-Kalabis, M., Li, L., Herlyn, M., 2014. Developmental pathways activated in melanocytes and melanoma. Arch. Biochem. Biophys 563, 13–21 Dec 1.

Masse, I., Barbollat-Boutrand, L., Kharbili, M.E., Berthier-Vergnes, O., Aubert, D., Lamartine, J., 2014. GATA3 inhibits proliferation and induces expression of both early and late differentiation markers in keratinocytes of the human epidermis. Arch. Dermatol. Res 306 (2), 201–208 Mar.

Marioni, J.C., Mason, C.E., Mane, S.M., Stephens, M., Gilad, Y., 2008. RNA-seq: an assessment of technical reproducibility and comparison with gene expression arrays. Genome Res. 18 (9), 1509–1517 Sep.

McCubrey, J.A., Steelman, L.S., Chappell, W.H., Abrams, S.L., Wong, E.W., Chang, F., Lehmann, B., Terrian, D.M., Milella, M., Tafuri, A., Stivala, F., Libra, M., Basecke, J., Evangelisti, C., Martelli, A.M., Franklin, R.A., 2007. Roles of the Raf/MEK/ERK pathway in cell growth, malignant transformation and drug resistance. Biochim. Biophys. Acta 1773 (8), 1263–1284 Aug.

Miyoshi, N., Ishii, H., Mimori, K., Nishida, N., Tokuoka, M., Akita, H., Sekimoto, M., Doki, Y., Mori, M., 2010. Abnormal expression of PFDN4 in colorectal cancer: a novel marker for prognosis. Ann. Surg. Oncol 17 (11), 3030–3036 Nov.

Moison, C., Assemat, F., Daunay, A., Tost, J., Guieysse-Peugeot, A.L., Arimondo, P.B., 2014. Synergistic chromatin repression of the tumor suppressor gene RARB in human prostate cancers. Epigenetics 9 (4), 477–482 Apr.

Mortazavi, A., Williams, B.A., McCue, K., Schaeffer, L., Wold, B., 2008. Mapping and quantifying mammalian transcriptomes by RNA-Seq. Nat. Methods 5 (7), 621–628 Jul.

Niizeki, H., Kobayashi, M., Horiuchi, I., Akakura, N., Chen, J., Wang, J., Hamada, J.I., Seth, P., Katoh, H., Watanabe, H., Raz, A., Hosokawa, M., 2002. Hypoxia enhances the expression of autocrine motility factor and the motility of human pancreatic cancer cells. Br. J. Cancer 86 (12), 1914–1919 Jun 17.

Nishino, J., Saunders, T.L., Sagane, K., Morrison, S.J., 2010. Lgi4 promotes the proliferation and differentiation of glial lineage cells throughout the developing peripheral nervous system. J. Neurosci 30 (45), 15228–15240 Nov 10.

Nordenberg, J., Aloni, D., Wasserman, L., Beery, E., Stenzel, K.H., Novogrodsky, A., 1985. Dimethylthiourea inhibition of melanoma cell growth in vitro and in vivo. J. Natl. Cancer Inst 75 (5), 891–895 Nov.

Nordenberg, J., Wasserman, L., Beery, E., Aloni, D., Malik, H., Stenzel, K.H., Novogrodsky, A., 1986. Growth inhibition of murine melanoma by butyric acid and dimethylsulfoxide. Exp. Cell Res 162 (1), 77–85 Jan.

Nordenberg, J., Wasserman, L., Peled, A., Malik, Z., Stenzel, K.H., Novogrodsky, A., 1987. Biochemical and ultrastructural alterations accompany the anti-proliferative effect of butyrate on melanoma cells. Br. J. Cancer 55 (5), 493–497 May.

Nordenberg, J., Wasserman, L., Gutman, H., Beery, E., Novogrodsky, A., 1989. Growth inhibition and induction of phenotypic alterations by L-histidinol in B16 mouse melanoma cells. Cancer Lett 47 (3), 193–197 Oct.

Nordenberg, J., Novogrodsky, A., Beery, E., Patia, M., Wasserman, L., Warshawsky, A., 1990. Anti-proliferative effects and phenotypic alterations induced by 8-hydroxyquinoline in melanoma cell lines. Eur. J. Cancer 26 (8), 905–907.

Obinata, A., Osakabe, K., Yamaguchi, M., Morimoto, R., Akimoto, Y., 2011. Tgm2/Gh, Gbx1 and TGF-beta are involved in retinoic acid-induced transdifferentiation from epidermis to mucosal epithelium. Int. J. Dev. Biol 55 (10−12), 933–943.

Park KH, Lee JW., Ryu YB, Ryu HW, Lee SA, Method for Screening Anti-cancer Compounds Inhibiting Functions of TM4SF5 and Anti-cancer Composition Containing Chalcone Compounds. KR20080052391, (2008).

Plisov, S., Tsang, M., Shi, G., Boyle, S., Yoshino, K., Dunwoodie, S.L., Dawid, I.B., Shioda, T., Perantoni, A.O., de Caestecker, M.P., 2005. Cited1 is a bifunctional transcriptional cofactor that regulates early nephronic patterning. J. Am. Soc. Nephrol 16 (6), 1632–1644 Jun.

Potop, I., Briese, A.M., Boeru, V., 1984. Research on the in vivo antitumoral action of thymosterin B in C57 black/6 mice implanted with melanoma B16 tumor. Endocrinologie 22 (2), 97–101 Apr-Jun.

Prohaska, J.R., Ganther, H.E., 1977. Interactions between selenium and methylmercury in rat brain. Chem. Biol. Interact 16 (2), 155–167 Feb.

Reed, J.A., Finnerty, B., Albino, A.P., 1999. Divergent cellular differentiation pathways during the invasive stage of cutaneous malignant melanoma progression. Am. J. Pathol 155 (2), 549–555 Aug.

Robles-Fernández, I., Rodríguez-Serrano, F., Álvarez, P.J., Ortiz, R., Rama, A.R., Prados, J., et al., 2013. Antitumor properties of natural compounds and related molecules. Recent Pat. Anticancer Drug Discov 8 (3), 203–215 Sep.

Roesch, A., 2015. Melanoma stem cells. J. Dtsch. Dermatol. Ges 13 (2), 118–124. http://dx.doi.org/10.1111/ddg.12584 Feb.

Saldanha, A.J., 2004. Java Treeview—extensible visualization of microarray data. Bioinformatics 20 (17), 3246–3248.

Schrottmaier, W.C., 2014. Oskolkova OV2, Schabbauer G3, Afonyushkin T4. MicroRNA miR-320a modulates induction of HO-1, GCLM and OKL38 by oxidized phospholipids in endothelial cells. Atherosclerosis 235 (1), 1–8 Jul.

Sell, S., 2005. Leukemia: stem cells, maturation arrest, and differentiation therapy. Stem Cell Rev. 1 (3), 197–205.

Semenza, G.L., 1998. Hypoxia-inducible factor 1: master regulator of O_2 homeostasis. Curr. Opin. Genet. Dev 8 (5), 588–594 Oct.

Semenza, G.L., 2011. Regulation of cancer cell metabolism by hypoxia-inducible factor 1. Cold Spring Harb. Symp. Quant. Biol 76, 347–353.

Storey, J.D., Tibshirani, R., 2003. Statistical significance for genomewide studies. Proc. Natl. Acad. Sci. U. S. A. 100 (16), 9440–9445 Aug 5.

Sun, L., Ma, K., Wang, H., Xiao, F., Gao, Y., Zhang, W., Wang, K., Gao, X., Ip, N., Wu, Z., 2007. JAK1-STAT1-STAT3, a key pathway promoting proliferation and preventing premature differentiation of myoblasts. J. Cell Biol 179 (1), 129–138 Oct 8.

Thewes, V., Orso, F., Jäger, R., Eckert, D., Schäfer, S., Kirfel, G., Garbe, S., Taverna, D., Schorle, H., 2010. Interference with activator protein-2 transcription factors leads to induction of apoptosis and an increase in chemo- and radiation-sensitivity in breast cancer cells. BMC Cancer 10, 192 May 11.

Walenta, S., Mueller-Klieser, W.F., 2004. Lactate: mirror and motor of tumor malignancy. Semin. Radiat. Oncol 14, 267–274.

Walenta, S., Schroeder, T., Mueller-Klieser, W., 2004. Lactate in solid malignant tumors: potential basis of a metabolic classification in clinical oncology. Curr. Med. Chem 11, 2195–2204.

Walle T, Halushka PV, A Method of Treating Colon Cancer by Administering Apigenin, Luteolin, Diosmetin and Crysin. WO2001058410, (2001).

Wang ZH, Sun C, Guo L, Liu JH, Wang T, Gan L, Wang XF, Li J, Zheng QS, Use of Isoliquiritigenin as Medicament for Preventing and Treating or Curing Postoperative Metastasis and Relapse of Malignant Tumors. CN101658513, (2010a).

Wang ZH, Li DF, Cheng HM, Fu W, Liu T, Zhang YK, Li J, Zheng QS, Application of Isoliquiritigenin as Cancer-differentiating Inducer. CN101627982, (2010b).

Wang, C., Zhang, B., Chen, N., Liu, L., Liu, J., Wang, Q., Wang, Z., Sun, X., Zheng, Q., 2015. Alteronol induces differentiation of melanoma b16-f0 cells. Recent Pat. Anticancer Drug Discov 10 (1), 116–127.

Watkins, J.F., Burns, G.B., Steplewski, Z., 1982. Studies on a human melanoma × hamster hybrid line selected by metastasis. Exp. Cell Biol 50 (1), 18–26.

Xu, L.L., Shi, Y., Petrovics, G., Sun, C., Makarem, M., Zhang, W., Sesterhenn, I.A., McLeod, D.G., Sun, L., Moul, J.W., Srivastava, S., 2003. PMEPA1, an androgen-regulated NEDD4-binding protein, exhibits cell growth inhibitory function and decreased expression during prostate cancer progression. Cancer Res 63 (15), 4299–4304 Aug 1.

Yang, D., Guo, J., Divieti, P., Shioda, T., Bringhurst, F.R., 2008. CBP/p300-interacting protein CITED1 modulates parathyroid hormone regulation of osteoblastic differentiation. Endocrinology 149 (4), 1728–1735 Apr.

Yoon, D.K., Jeong, C.H., Jun, H.O., Chun, K.H., Cha, J.H., Seo, J.H., Lee, H.Y., Choi, Y.K., Ahn, B.J., Lee, S.K., Kim, K.W., 2007. AKAP12 induces apoptotic cell death in human fibrosarcoma cells by regulating CDKI-cyclin D1 and caspase-3 activity. Cancer Lett 254 (1), 111–118 Aug 28.

Zhao, X., Murata, T., Ohno, S., Day, N., Song, J., Nomura, N., Nakahara, T., Yokoyama, K.K., 2001. Protein kinase Calpha plays a critical role in mannosylerythritol lipid-induced differentiation of melanoma B16 cells. J. Biol. Chem 276 (43), 39903–39910 Oct 26.